Novel insights into enzymes inhibitory responses and metabolomic profile of supercritical fluid extract from chestnut shells upon intestinal permeability

Diana Pinto [a], Julián Lozano-Castellón [b,c], Ana Margarida Silva [a], María de la Luz Cádiz-Gurrea [d], Antonio Segura-Carretero [d], Rosa Lamuela-Raventós [b,c], Anna Vallverdú-Queralt [b,c,*], Cristina Delerue-Matos [a], Francisca Rodrigues [a,*]

[a] REQUIMTE/LAQV, ISEP, Polytechnic of Porto, Rua Dr. António Bernardino de Almeida, 4249-015 Porto, Portugal
[b] Nutrition, Food Science and Gastronomy Department, School of Pharmacy and Food Science, University of Barcelona, 08028 Barcelona, Spain
[c] Consorcio CIBER, M.P. Fisiopatología de la Obesidad y la Nutrición (CIBERObn), Instituto de Salud Carlos III (ISCIII), 28029 Madrid, Spain
[d] Department of Analytical Chemistry, Faculty of Sciences, University of Granada, Avenida Fuentenueva s/n, 18071 Granada, Spain

ARTICLE INFO

ABSTRACT

The health benefits of chestnut (*Castanea sativa*) shells (CSs) have been ascribed to phytochemicals, mainly phenolic compounds. Nevertheless, an exhaustive assessment of their intestinal absorption is vital considering a possible nutraceutical application. This study evaluated the bioactivity of CSs extract prepared by Supercritical Fluid Extraction and untargeted metabolomic profile upon *in-vitro* intestinal permeation across a Caco-2/HT29-MTX co-culture model. The results demonstrated the neuroprotective, hypoglycemic, and hypolipidemic properties of CSs extract by inhibition of acetylcholinesterase, α-amylase, and lipase activities. The untargeted metabolic profiling by LC-ESI-LTQ-Orbitrap-MS unveiled almost 60 % of lipids and 30 % of phenolic compounds, with 29 metabolic pathways indicated by enrichment analysis. Among phenolics, mostly phenolic acids, flavonoids, and coumarins permeated the intestinal barrier with most metabolites arising from phase I reactions (reduction, hydrolysis, and hydrogenation) and a minor fraction from phase II reactions (methylation). The permeation rates enhanced in the following order: ellagic acid < *o*-coumaric acid < *p*-coumaric acid < ferulaldehyde ≤ hydroxyferulic acid ≤ dihydroferulic acid < ferulic acid < *trans*-caffeic acid < *trans*-cinnamic acid < dihydrocaffeic acid, with better outcomes for 1000 μg/mL of extract concentration and after 4 h of permeation. Taken together, these findings sustained a considerable *in-vitro* intestinal absorption of phenolic compounds from CSs extract, enabling them to reach target sites and exert their biological effects.

1. Introduction

Over the last decades, phenolic compounds have emerged as fascinating bioactive compounds, acting as antioxidants, antimicrobial, anti-inflammatory, and disease-preventing agents (Cádiz Gurrea et al., 2019; Pinto, Cádiz-Gurrea, Vallverdú-Queralt, Delerue-Matos, & Rodrigues, 2021) with outstanding versatility and encompassing a broad range of applications from biomedicine to dietary supplementation (Rocchetti et al., 2020). These phytochemicals have been found in diverse foods and by-products, including chestnut (*Castanea sativa* Mill.) shells (CSs).

Chestnut is an appealing fruit commercially exploited all over the world, particularly on a larger scale in southern Europe (Pinto et al., 2020; Pinto et al., 2021), owing to its beneficial impacts on human health attributed to the high content of phenolic compounds (Pérez et al., 2017; Sangiovanni et al., 2018; Yuan et al., 2022; Zhang, Yang, Liu, Wu, & Ouyang, 2020). Folk medicine has claimed the traditional use of different parts of *C. sativa* plant to treat cough, diarrhea, and infertility (Neves, Matos, Moutinho, Queiroz, & Gomes, 2009). In the last decade, deep attention has been given to CSs owing to its phytochemical composition rich in phenolic acids, flavonoids, lignans, and vitamin E,

which has been documented by different reports (Lameirão et al., 2020; Pinto et al., 2023; Pinto et al., 2020; Pinto et al., 2020; Pinto et al., 2023; Pinto et al., 2023; Pinto et al., 2021; Pinto et al., 2021; Rodrigues et al., 2015). These bioactive molecules have potential *in-vivo* pro-healthy effects, comprising excellent candidates for the development of nutraceutical products, especially endowed with antioxidant properties (Pinto et al., 2023; Pinto et al., 2023). Despite the legislation for the validation of new nutraceutical ingredients remains unclear, an in-depth assessment of the bioaccessibility, bioavailability and *in-vivo* health benefits of these molecules is vital due to the biochemical reactions that occur during digestion and absorption (Martins, Barros, & Ferreira, 2016; Pinto et al., 2023). A recent study from our research group has optimized the extraction of phenolic compounds from CSs by Supercritical Fluid Extraction (SFE) using a central composite design (CCD), achieving the optimal extract at 60 °C, 350 bar and 15 % of ethanol (co-solvent) (Pinto et al., 2020). Ellagic acid, epigallocatechin, caffeic acid derivative, catechin, apigenin-7-*O*-rutinoside, luteolin-7-*O*-rutinoside, and proanthocyanidins were identified as the main phenolic compounds responsible for the antioxidant/antiradical properties observed. The absence of toxicity on intestinal cells ensures the extract safety up to 100 μg/mL (Pinto et al., 2020). Nevertheless, phenolic compounds must be bioavailable to exert their therapeutical effects on target cells or tissues (Hu et al., 2023; Pan, Li, Shahidi, Luo, & Deng, 2022). Their bioavailability depends on their bioaccessibility (i.e., the concentration of compounds released from the food matrix in the active form), providing insights into their absorption, tissue distribution, metabolism, and excretion (Crozier, Del Rio, & Clifford, 2010; Fernández-Ochoa et al., 2022). The bioavailability evaluated by clinical and animal studies raises ethical concerns and other challenges (Crozier et al., 2010; Martins et al., 2016). Alternatively, *in-vitro* cellular models have been implemented to appraise the intestinal permeability and the absorption of phenolic compounds, enabling the reproducibility of complex transport mechanisms and morphological characteristics (Martinelli et al., 2021; Martins et al., 2016). These methods are low cost, less laborious, and without ethical considerations (Martinelli et al., 2021). Several models have been proposed to simulate the intestinal absorption of phytochemicals and predict their bioavailability, including Caco-2 cell monolayers, Caco-2/HT29-MTX co-culture, and Caco-2/HT29-MTX/ Raji B triple culture models (Araújo & Sarmento, 2013; de Francisco et al., 2018; González et al., 2019; Herrera-Balandrano et al., 2023). Caco-2 cells mimic the human colon owing to the presence of microvilli, tight junctions, transporters, nuclear receptors and enzymes, while HT29-MTX cells simulate the goblet cells useful for the evaluation of the mucoadhesion of carrier systems (Araújo & Sarmento, 2013). In addition, the combination of cell-based assays with metabolomic approaches allow to identify potential biomarkers of phenolic compounds correlated to therapeutical effects and, consequently, predicting their *in-vivo* bioactivity (Martinelli et al., 2021).

This work aims to investigate the phytochemical composition of CSs extract prepared by SFE through liquid chromatography coupled to Orbitrap-mass spectrometry (LC-ESI-LTQ-Orbitrap-MS) and to evaluate its *in-vitro* intestinal permeation through a Caco-2/HT29-MTX co-culture model, considering its validation as a new nutraceutical ingredient. The bioactivity of CSs extract was assessed by inhibitory responses on acetylcholinesterase (AChE), α-amylase, and lipase activities. Enrichment analysis was performed to elucidate the metabolic pathways of the annotated compounds. To the best of our knowledge, this is the first study that estimates the permeation rate of a phenolics-rich SFE extract from CSs across an intestinal model using an untargeted metabolomic approach.

2. Materials and methods

2.1. Chemicals

All chemicals, solvents, and standards were of analytical reagent grade, used as received or dried by standard procedures, and purchased from commercial sources. Dulbecco's modified Eagle medium (DMEM), fetal bovine serum (FBS), Hank's balanced salt solution (HBSS), non-essential amino acids, penicillin, streptomycin, and trypsin–EDTA were acquired from Invitrogen Corporation (Life Technologies, S.A., Madrid, Spain). Standards used for the metabolomic analyses were acquired as follows: apigenin, caffeic acid, (+)-catechin, (−)-epicatechin, and ellagic acid from Sigma-Aldrich (Steinhemin, Germany); delphinidin-3-*O*-sambubioside and cyanidin-3-*O*-sambubioside-5-*O*-glucoside from Extrasynthèse (Genay, France). All other chemicals were provided by Sigma-Aldrich (Steinhemin, Germany). HPLC grade solvents, namely acetonitrile, ethanol, and formic acid, were supplied by Merck (Darmstadt, Germany). Ultrapure water was obtained from a Milli-Q water purification system (Millipore Bedford, MA, USA).

2.2. Sample

CSs were generously offered by Sortegel (Sortes, Bragança, Portugal) in October 2018. After dehydration at 40 °C for 24 h (Excalibur Food Dehydrator, USA), shells were ground to 1 mm of particle size using an ultra-centrifugal grinder (Retsch ZM200, Germany) and stored in sealed flasks at room temperature in the dark.

2.3. Extraction of phenolic compounds by supercritical fluid extraction

The phenolic compounds were extracted using a supercritical fluid extractor (Waters Prep Supercritical Fluid Extraction System SFE-100, Milford, MA, USA) attached to automated back pressure regulator, CO_2 and co-solvent pumps, heating exchangers for low and high pressures, and collection vessels as described by Pinto et al. (2020). The extraction vessel contained a three-layer sandwich. The first and third layers were composed of 5 g of Ottawa sand. The powdered dried shells (15 g) were blended with Ottawa sand (30 g) comprising the second layer. A Accel 500 LC chiller (Thermo Scientific™, Leicestershire, UK) was used to maintain CO_2 in the liquid state. Wool glass (Sigma-Aldrich, Steinheim, Germany) was added at the top and bottom of the extraction cell to avoid sample projection. CO_2 (Air Product and Chemicals, Allentown, PA, USA) and ethanol (VWR chemicals, Radnor, PA, USA) were used, respectively, as supercritical fluid and co-solvent. The extraction conditions were set at 60 °C, 350 bar, and 15 % of ethanol (co-solvent) based on a previous optimization study from our research group (Pinto et al., 2020). A steady flow rate of 30 g/min was applied during 90 min. Three independent extractions were performed. Finally, the extract was evaporated (Rotavapor Buchi R210, Flawil, Switzerland) and kept at −20 °C in the dark.

2.4. In-vitro biological activities

For the enzymes inhibitory assays, three concentrations of CSs extract were selected (namely between 12.5 and 300 μg/mL), aiming to investigate a broad range of concentrations and attempting to determine the IC_{50} values.

2.4.1. Acetylcholinesterase (AChE) activity inhibition

The AChE activity was evaluated by a commercial enzymatic kit (Sigma-Aldrich, St. Louis, USA) based on the reaction between 5,5′-dithiobis(2-nitrobenzoic acid) and thiocholine and the formation of a colorimetric product with maximum absorbance at 412 nm (Pinto et al., 2023; Pinto et al., 2021). The results were expressed as inhibition percentage (%).

2.4.2. α-amylase activity inhibition

The α-amylase activity was evaluated by a commercial enzymatic kit (Sigma-Aldrich, St. Louis, USA) based on the cleavage of ethylidene-pNP-G7 (used as substrate) and the formation of a colorimetric product with maximum absorbance at 405 nm (Pinto et al., 2023; Pinto et al.,

2021). The standard used was nitrophenol and the results were expressed as inhibition percentage (%).

2.4.3. Lipase activity inhibition

The lipase activity was evaluated by a commercial kit (Sigma-Aldrich, St. Louis, USA) through a coupled enzymatic reaction, producing glycerol from triglycerides with a maximum absorbance at 570 nm (Pinto et al., 2023; Pinto et al., 2021). The standard used was glycerol and the results were expressed as inhibition percentage (%).

2.5. In-vitro intestinal permeability

2.5.1. Cell culture

Caco-2 (ATCC Number: HTB-37; age, 72 years; sex, male; ethnicity, Caucasian; tissue, colon) and HT29-MTX (ATCC Number: HTB-38; ethnicity, Caucasian; age, 44 years; sex, female; tissue, colon) cells were supplied by the American Type Culture Collection (ATCC, Manassas, VA, USA). A complete medium of DMEM supplemented with 10 % (*v/v*) FBS, 1 % (*v/v*) antibiotic–antimitotic mixture (containing 100 U/mL penicillin and 100 U/mL streptomycin), 1 % (*v/v*) *L*-glutamine, and 1 % (*v/v*) non-essential amino acids was used. Caco-2 and HT29-MTX cells were seeded individually in tissue culture flasks (Orange Scientific, Belgium) and cultivated at 37 °C in an incubator with 5 % CO_2 environment (CellCulture® CO_2 Incubator, ESCO GB Ltd., Barnsley, UK). Every 48 h the cells were washed with HBSS and supplied with fresh medium. Both cells were harvested at 90–95 % confluence using trypsin.

2.5.2. Caco-2/HT29-MTX cells co-culture model

Caco-2 (passage 70–71) and HT29-MTX (passage 33–34) cells were cultivated for 21 days in a proportion of 90:10 (at density of 1×10^5 cells/cm^2) in the apical compartment of 12-well Transwell® plates (3 μm pore diameter, polycarbonate, 1.12 cm^2). The culture medium was changed every 48 h. After 21 days, the culture medium was removed, and cell monolayers were washed twice with HBSS at 37 °C. Two CSs extract concentrations (100 and 1000 μg/mL) dissolved in HBSS were selected for testing the intestinal permeability based on the cell viability results in Caco-2 and HT29-MTX published in our previous paper (Pinto et al., 2020). Aliquots of 200 μL were collected from the basolateral compartment at fixed times (0, 15, 30, 45, 60, 90, 120, 180, and 240 min). The same volume of HBSS was added. A negative control with HBSS was analyzed. The procedure was conducted at 37 °C. The cells monolayer integrity was monitored during the cell culture and assay by measuring the transepithelial electrical resistance (TEER) using an EVOM epithelial voltmeter with electrodes (World Precision Instruments, Sarasota, FL, USA). The permeated samples collected at fixed time-points were further analyzed by LC-ESI-LTQ-Orbitrap-MS following the methodology applied in previous studies from our research group (Escobar-Avello et al., 2021; Pinto et al., 2023; Pinto et al., 2023; Pinto et al., 2023) and using data processing MS-finder and MS-dial software (described in detail in sections 2.6 and 2.7) for untargeted and targeted metabolomic profiling. The assay was performed in triplicate according to Pinto et al. (2021). The results of the metabolomic studies targeted on phenolic compounds are expressed as the percentage of each phenolic compound or metabolite permeated across the intestinal model barrier from the donor to the recipient compartment (at each time). The apparent permeability coefficient (P_{app}) was determined using the following equation (1):

$$P_{app}(cm/s) = (dQ/dt) \times A \times C_0 \tag{1}$$

Where dQ represents the amount of permeated compound (μg), dt represents the time of collection (s), A represents the diffusion Transwell® area (cm^2), and C_0 represents the initial concentration of the compound (μg/mL).

2.6. Untargeted metabolomic profile by LC-ESI-LTQ-Orbitrap-MS

The untargeted metabolic analysis of CSs extract and permeated samples was performed following the methodologies proposed in our previous studies (Escobar-Avello et al., 2021; Lozano-Castellón et al., 2022; Pinto et al., 2023), with minor modifications. The equipment used was a LC-ESI-LTQ-Orbitrap-MS equipped with an Accela chromatograph (Thermo Scientific, Hemel Hempstead, UK), a photodiode array detector, a quaternary pump, and a thermostated autosampler attached to LTQ Orbitrap Velos mass spectrometer (Thermo Scientific, Hemel Hempstead, UK) with an ESI source in negative mode. Xcalibur v3.0 software (ThermoFisher Scientific, Hemel Hempstead, UK) was used for the system control. The elution was conducted using an Acquity™ UPLC® BEH C18 Column (2.1 × 100 mm, i.d., 1.7 μm particle size, Waters Corporation, Wexford, Ireland) maintained at 30 °C. The solvents used were water containing 0.1 % formic acid (A) and acetonitrile containing 0.1 % formic acid (B). The solvent gradient of B was 0 min, 6 % B; 0–29 min, 94 % B; 29–32 min, 94 % B; 32–35 min, 6 % B. The column was equilibrated for 5 min returning to initial conditions. The column temperature was set at 30 °C. Flow rate and injection volume were established, respectively, at 0.250 mL/min and 10 μL. The instrumental conditions were defined according to Escobar-Avello et al. (2021) and Pinto et al. (2023). Samples were studied in full scan mode at 30,000 of resolving power and *m/z* 600 with data-dependent MS/MS events attained at 15,000 of resolving power. The ions with high intensity were determined in FTMS mode-triggered data-dependent scanning. The lower intensity ions were detected by MS^n mode for a data-dependent scan. The precursors fragmentation was conducted by collision-induced dissociation with a C-trap normalized collision energy (35 V) and 10 ms of activation time. The chromatographic features were established as follows: auxiliary gas, 20 a.u.; capillary temperature, 375 °C; sheath gas, 50 a.u. (arbitrary units); source voltage, 3 kV; and sweep gas, 2 a.u.

The putative identification of compounds was done by annotation using MS-finder software and MS-dial software (open source software version 4 developed by Prof. Masanori Arita team (RIKEN) and Prof. Oliver Fiehn team (UC Davis) supported by the JST/NSF SICORP "Metabolomics for the low carbon society" project, Wakō, Japan, and Sacramento, CA, USA) for data treatment, regarding the high confidence provided by the fragmentation pattern, isotopic pattern (isotopic spacing and isotopic ratio) followed by exact mass, and retention time alignments. A database set resulting from a combination of annotations from Phenol-Explorer (https://phenol-explorer.eu/ (accessed on 14 March 2022)) and Food Database (https://foodb.ca/ (accessed on 14 March 2022)) was used as reference for putative annotation.

2.7. Quantification of phenolic compounds and metabolites

The quantitative analysis was performed according to the chromatographic method validated by our research group in a previous study (Laveriano-Santos et al., 2022). The following commercial standards were tested for the quantification of phenolic compounds by LC-ESI-LTQ-Orbitrap-MS: caffeic acid, apigenin, catechin, epicatechin, ellagic acid, delphinidin-3-*O*-sambubioside, and cyanidin-3-*O*-sambubioside-5-*O*-glucoside. The respective phenolic compounds and metabolites (whose standards were not available) were identified considering the chemical composition, elution time, accurate masses, MS/MS fragmentation and isotopic patterns, and comparing with similar standard compounds. The quantification of phenolic compounds was performed using the standards calibration curves (concentration range = 1–10 μg/mL). Semi-quantification was conducted for the remaining phenolic compounds and metabolites. The phenolic metabolites were quantified based on the calibration curves of the parent compounds that originated them. The calculations were performed based on the peak area of the parent molecules. The standard calibration curves were as follows:

$$Caffeic\ acid:\ y = 207337x - 92910\ \left(R^2 = 0.8614\right)$$

$$Apigenin:\ y = 2210313x + 12144253\ \left(R^2 = 0.9636\right)$$

$$(+) - Catechin:\ y = 1431186x + 1247435\ \left(R^2 = 0.9699\right)$$

$$(-) - Epicatechin:\ y = 1859674x + 2053835\ \left(R^2 = 0.9585\right)$$

$$Ellagic\ acid:\ y = 68932x + 8028\ \left(R^2 = 0.8057\right)$$

$$Delphinidin - 3 - O - sambubioside:\ y = 8368x + 28001(R^2 = 0.9725)$$

$$Cyanidin - 3 - O - sambubioside - 5 - O - glucoside:\ y$$
$$= 50547x - 70863\ \left(R^2 = 0.8897\right)$$

Considering CSs extract, the results are expressed in μg of each phenolic compound equivalent per mg on DW (μg/mg DW). Regarding permeated samples, the results are expressed as the permeation percentage of each phenolic compound across the intestinal barrier (at each time).

2.8. Statistical analysis

Three independent experiments were performed for each assay. IBM SPSS Statistics 24.0 software (Chicago, IL, USA) was used for statistical analysis by one-way ANOVA and Tukey's HSD test, denoting a $p < 0.05$

for significant differences. MetaboAnalyst v5.0 software was employed for enrichment analysis to predict the metabolic pathways of the annotated compounds.

3. Results and discussion

3.1. Enzymes inhibitory responses

The *in-vitro* bioactivity of CSs extract prepared by SFE was evaluated on AChE, α-amylase, and lipase activities (Fig. 1). For the enzymes activity assays, low extract concentrations (between 12.5 and 300 μg/mL) were tested to ascertain if these concentrations are capable of inhibiting the enzymes activities.

AChE is the cholinergic enzyme mainly found at postsynaptic neuromuscular junctions, being implicated in the hydrolysis of the neurotransmitter acetylcholine (ACh). AChE inhibitors (e.g., galantamine) are effective drugs in the therapy of dementia and neurodegenerative pathologies (i.e., Alzheimer's and Parkinson's diseases) by decreasing AChE activity and ameliorating cognitive functions (Pinto et al., 2021). Alternatively, neuroprotective effects have been proven for bioactive molecules extracted from natural products (i.e., alkaloids, flavonoids, and terpenoids), proposing their use for the prevention/cotherapy of early and moderate stage of neurodegenerative diseases to avoid the side effects of synthetic drugs (Pinto et al., 2023; Wojdyło, Turkiewicz, Tkacz, Nowicka, & Bobak, 2022). The anticholinergic activity of CSs extract enhanced from 26 % (at 12.5 μg/mL) to 64 % (at 50

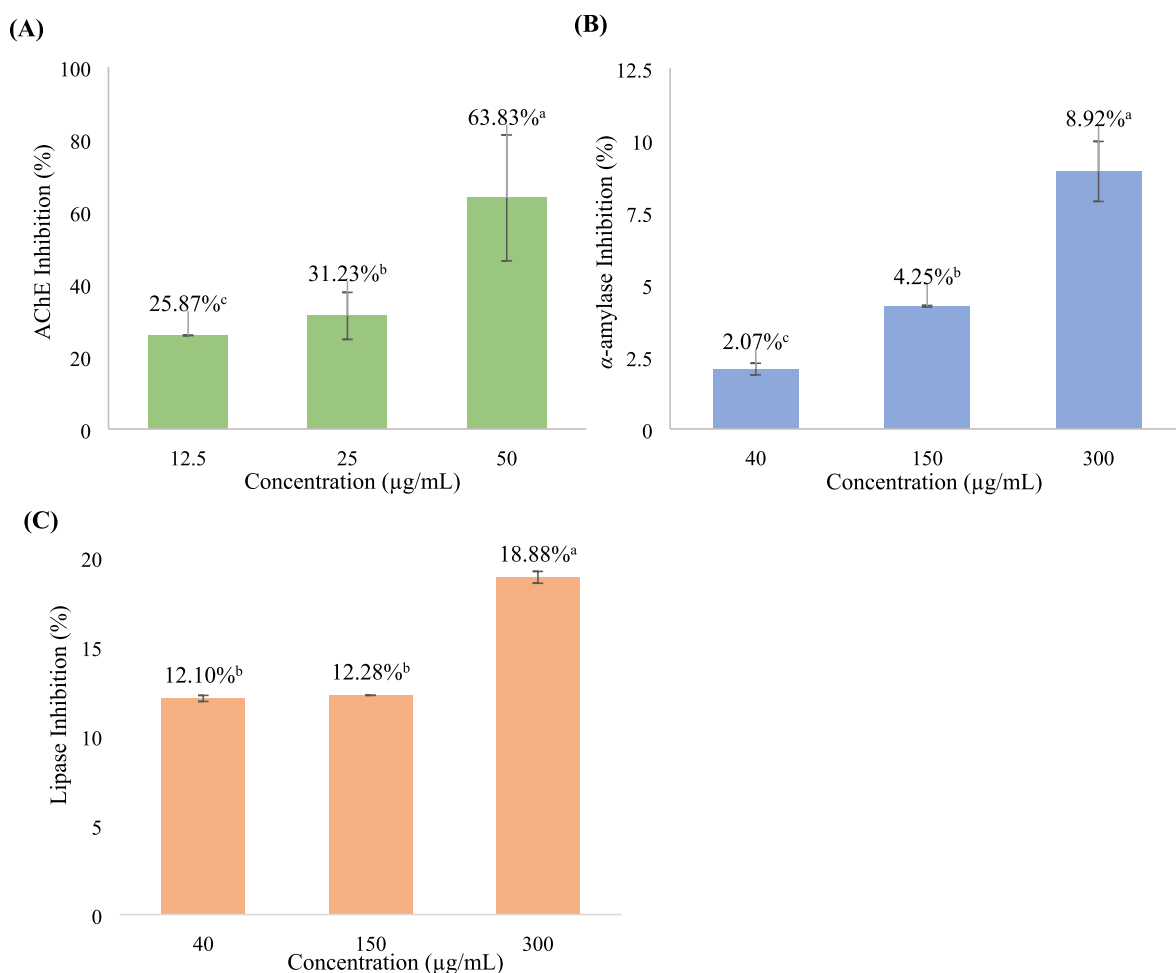**Fig. 1.** Inhibition of AChE (A), α-amylase (B), and lipase (C) activities of different concentrations (12.5 – 300 μg/mL) from CSs extract prepared by SFE ($n = 3$). Different letters (a, b, and c) denote significant differences ($p < 0.05$) between samples.

μg/mL) of AChE inhibition, with significant differences ($p < 0.05$) between concentrations (Fig. 1A). The IC$_{50}$ value was 39.39 μg/mL. Recently, Wojdyło et al. (2022) investigated the role of nuts as functional foods considering their phytochemical composition and *in-vitro* bioactivity. Lower AChE inhibitory responses were attained for pecan, pine, hazelnuts, pistachio, almonds, cashew, walnuts, and macadamia, with values ranging between 8.1 % and 29.1 %, achieving better results for pecan nuts. The anti-cholinergic activities of nuts were explained by the abundance of flavonols, triterpenes, and polyunsaturated fatty acids with a r^2 up to 0.6 (Wojdyło et al., 2022).

Considering the anti-diabetic potential, α-amylase activity encompasses the hydrolysis of glucan linkages in polysaccharides. An increased α-amylase activity is a strong indicator of pancreatic disorders, mainly diabetes, which represents a huge impact in health and economy sector (Gamboa-Gómez et al., 2017; Wojdyło et al., 2022). Although α-amylase inhibitory drugs (e.g., acarbose) are widely employed in the therapy of type II diabetes to reduce the post-prandial blood glucose levels, natural molecules have been exploited as complementary antidiabetic agents (Gamboa-Gómez et al., 2017; Pinto et al., 2023; Wojdyło et al., 2022). The anti-amylase activity of CSs extract was almost 9 % (at 300 μg/mL) (Fig. 1B), with significant differences ($p < 0.05$) being observed between the concentrations tested. According to Gamboa-Gómez et al. (2017), identical inhibitions were obtained for *Quercus arizonica* and *Q. convallata* leaves infusions and fermented beverages (<10 % inhibition). Furthermore, Wojdyło et al. (2022) reported higher α-amylase inhibition for different nuts, varying between 26.8 % and 60.7 %, respectively, for pistachio and pecan, being these results mostly ascribed to flavonols ($r^2 = 0.70$). Nevertheless, higher concentrations of nut extracts (1 mg/mL) prepared using methanol/water/hydrochloric acid (80:19:1, $v/v/v$) as solvent were tested, explaining the better outcomes obtained (Wojdyło et al., 2022).

The anti-obesity effects of natural extracts have been explored by inhibition of lipase activity involved in lipids metabolism, inflammation and cell signaling (Pinto et al., 2023, Pinto et al., 2021). The lipase activity is a useful marker of metabolic pathologies, such as Crohn's, celiac and pancreatic diseases as well as cystic fibrosis (Pinto et al., 2021). Beyond orlistat, used as first line drug, natural extracts have been proposed as alternative lipase inhibitors, with their use being recommended for obesity (Pinto et al., 2023; Pinto et al., 2021; Wojdyło et al., 2022). The anti-lipase activity of CSs extract enhanced from 12 % to 19 % inhibition, respectively, at 40 and 300 μg/mL (Fig. 1C). Significant differences ($p < 0.05$) were only attained for the highest concentration. Wojdyło et al. (2022) demonstrated better anti-lipase effects for all nuts analyzed, with inhibition percentages varying from 36.3 % to 127.2 %, respectively, for almonds and pecan. The correlations highlighted the outstanding contribution of phenolic acids ($r^2 = 0.64$) and tocotrienols ($r^2 = 0.57$) to these results. Notwithstanding, the higher concentrations of nut extracts analyzed in this study may justify the discrepancies on the results (Wojdyło et al., 2022).

The promising results obtained emphasize mild to strong neuroprotective, hypoglycemic and hypolipidemic properties for CSs extract prepared by SFE, probably due to the phenolic composition, namely ellagic, *o*-coumaric, *p*-coumaric, ferulic, *trans*-caffeic, and *trans*-cinnamic acids, whose enzyme inhibitory effects were already proven in recent studies (Aloo, Ofosu, Kim, Kilonzi, & Oh, 2023; Fatima, Bhat, Nisar, Fakhro, & Al-Shabeeb Akil, 2023; Szwajgier, Borowiec, & Pustelniak, 2017). Notably, the bioactivity of CSs extract prepared by SFE on AChE, α-amylase, and lipase was not previously evaluated, remaining an unexploited research field. In summary, the proven enzymes inhibitory properties highlight mild to strong bioactivity using low extract concentrations.

3.2. Untargeted metabolomic profiling by LC-ESI-LTQ-Orbitrap-MS

The untargeted metabolomic profiling of CSs extract and respective permeated samples was explored by LC-ESI-LTQ-Orbitrap-MS to outline

modifications in the phytochemical composition upon *in-vitro* intestinal permeability model. **Supplementary Table 1** presents the putative annotation of compounds, while **Supplementary Table 2** provides a detailed identification list of the compounds presumptively annotated in CSs extract and the permeated samples.

Considering the CSs extract, a total of 112 compounds were putatively annotated at 1000 μg/mL, with a higher abundance of lipids (66 compounds, representing 58.9 %) and polyphenols (32 compounds, representing 28.6 %), followed by organic acids (8 compounds, representing 7.1 %), carbohydrates (4 compounds, representing 3.6 %), amino acids and derivatives (1 compound, representing 0.9 %), and alcohols or polyols (1 compound, representing 0.9 %). Only 82 compounds were presumptively annotated at 100 μg/mL, including 53 lipids (representing 64.6 %), 21 polyphenols (25.6 %), 5 organic acids (6.1 %), and 3 carbohydrates (3.7 %). Alcohols or polyols and amino acids were not identified at the lowest tested concentration (100 μg/mL). Among lipids, fatty acyls are the most abundant subclass, representing up to 57.6 % of the total lipids annotated, followed by prenol lipids/terpenoids (33.3 %), steroids (3.0 %), saccharolipids (3.0 %), glycerolipids (1.5 %), and glycerophospholipids (1.5 %). Concerning polyphenols, phenolic acids are the major class with up to 39.0 %, followed by flavonoids (26.8 %). The phenolic acids identified were hydroxycinnamic acids (HCAs), with up to 50 % of the total phenolic acids, hydroxybenzoic acids (HBAs, 31.25 %), hydroxyphenylacetic acids (HPAAs, 12.5 %), and hydroxyphenylpropanoic acids (HPPAs, 6.25 %). Among flavonoids, *O*-methylated flavonoids were the most abundant (up to 36.4 % of the total flavonoids), followed by flavones (27.3 %), flavanones (18.2 %), dihydrochalcones (9.1 %) and isoflavonoids (9.1 %). Furthermore, other polyphenols were annotated with less abundance, including hydroxycoumarins (7.3 %), benzenediols (7.3 %), hydroxybenzaldehydes (4.9 %), methoxyphenols (4.9 %), hydrolysable tannins (2.4 %), isocoumarins (2.4 %), alkylphenols (2.4 %), diarylheptanoids (2.4 %), and hydroxycinnamaldehydes (2.4 %). In summary, the CSs extract prepared by SFE is mainly composed by lipids and polyphenols. SFE is an efficient technique for the extraction of lipophilic compounds (e.g., carotenoids, fatty acids, phytosterols, some polyphenols, tocopherols, and triglycerides) from foods and by-products due to the high affinity of CO_2 (used as extraction solvent) for non-polar molecules (Pimentel-Moral et al., 2019; Pinto et al., 2020). This feature may explain the abundance of fatty acids, esters, sugar moieties and some lipophilic polyphenols in CSs extract.

Regarding the permeated samples, the results demonstrated a higher abundance of compounds annotated after permeation of the highest CSs extract concentration tested (1000 μg/mL) across the intestinal barrier. Moreover, the number of compounds detected increased with the increase of the exposure time during the intestinal permeability assay. After 4 h of assay, a total of 69 and 99 compounds were annotated, respectively, in the permeated samples of CSs extract at 100 and 1000 μg/mL. In contrast, only 26 and 45 compounds were tentatively annotated after 15 min of permeation, respectively, at 100 and 1000 μg/mL. Phenolics and lipids correspond to, at least, 90 % of the total number of compounds annotated in the permeated samples.

3.3. Metabolic pathways analysis

The metabolic pathways were studied by enrichment analysis considering the untargeted metabolic profile (**Supplementary Table 1**) using MetaboAnalyst v5.0 software (Fig. 2).

The Kyoto Encyclopedia of Genes and Genomes (KEGG) enrichment analysis unveiled 29 metabolic pathways. The most relevant pathways include α-linolenic and linoleic acids metabolism (for 19 compounds identified), phenylacetate metabolism (9 compounds), trehalose degradation (11 compounds), ketone body metabolism (13 compounds), butyrate metabolism (19 compounds), mitochondrial electron transport chain (19 compounds), ubiquinone biosynthesis (20 compounds), glutathione metabolism (21 compounds), carnitine synthesis (22
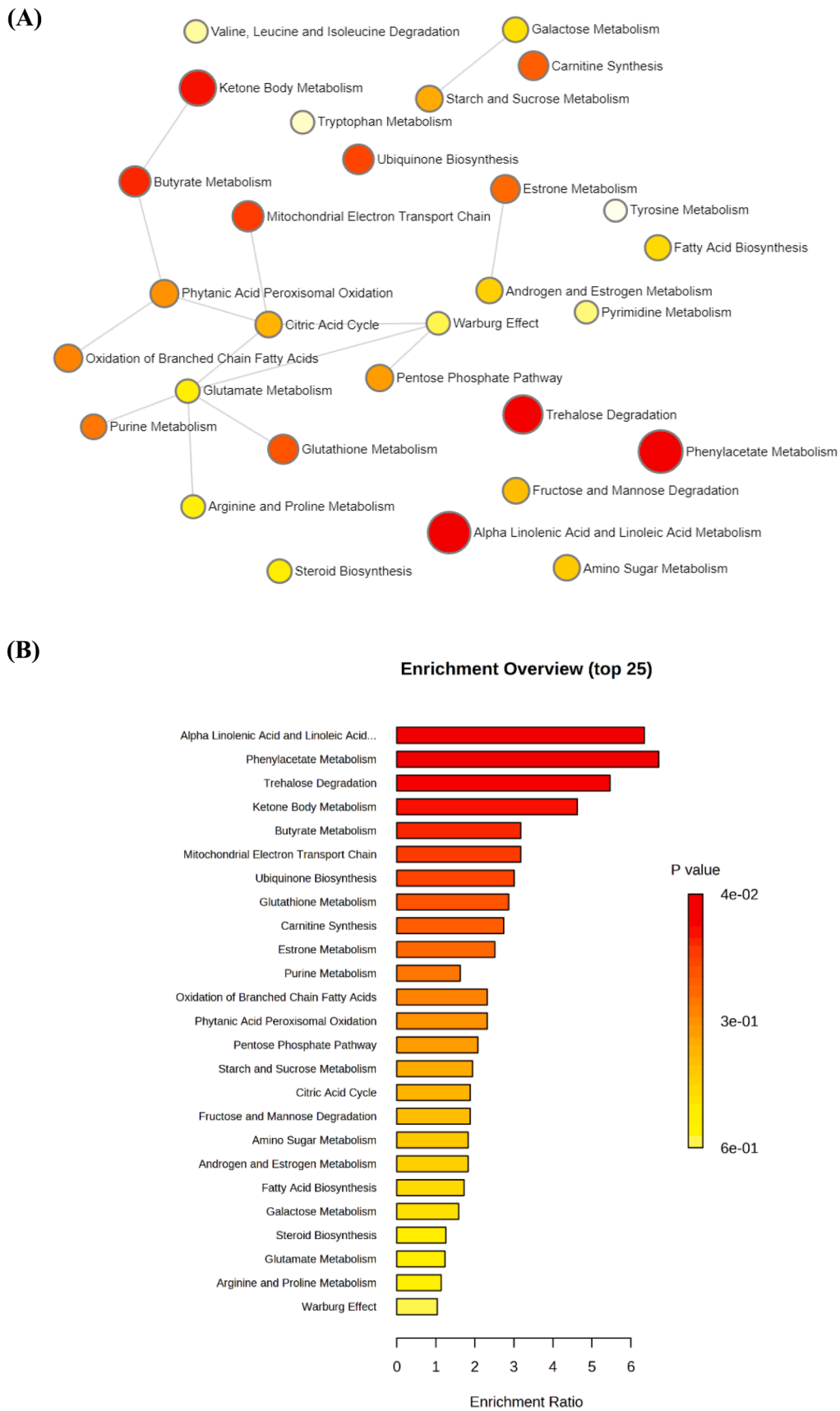
(A)

(B)

Fig. 2. Enrichment analysis of annotated compounds in the permeated samples using MetaboAnalyst platform.

compounds), estrone metabolism (24 compounds), purine metabolism (74 compounds), oxidation of branched chain fatty acids (26 compounds), phytanic acid peroxisomal oxidation (26 compounds), and pentose phosphate pathway (29 compounds) with *p*-values lower than 0.5. Other pathways influencing the metabolic profiling encompass starch and sucrose metabolism (31 compounds), citric acid cycle (32 compounds), fructose and mannose degradation (32 compounds), amino sugar metabolism (33 compounds), androgen and estrogen metabolism (33 compounds), fatty acid biosynthesis (35 compounds), galactose metabolism (38 compounds), steroid biosynthesis (48 compounds), glutamate metabolism (49 compounds), arginine and proline metabolism (53 compounds), warburg effect (58 compounds), pyrimidine metabolism (59 compounds), valine, leucine and isoleucine degradation (60 compounds), tryptophan metabolism (60 compounds), and tyrosine metabolism (72 compounds).

3.4. Identification and quantification of phenolic compounds in CSs extract

Over the past decade, scientific research has evidenced the role of plant-based foods and their by-products as sources of biologically active molecules useful in a healthy lifestyle, preventing chronic disorders, delaying premature aging, and delivering innumerable other health benefits (Cádiz Gurrea et al., 2019; Pinto, Delerue-Matos, & Rodrigues, 2020; Pinto et al., 2024). Recent studies have demonstrated the high nutritional value and wealth of CSs in antioxidants (i.e., polyphenols and vitamin E), proposing a correlation with their *in-vitro* biological properties (Pinto et al., 2023; Pinto et al., 2021; Pinto et al., 2020; Pinto et al., 2023; Pinto et al., 2023; Pinto et al., 2023; Pinto et al., 2021; Rodrigues et al., 2015). Notwithstanding, the intestinal absorption of phenolic-rich CSs extract obtained by SFE has not yet been investigated, highlighting the novelty of the current study.

In a previous study, our research team optimized the antioxidants extraction from CSs using the same extraction technique and conditions employed in this study and providing a preliminary study on the phytochemical composition of the optimal CSs extract by ^{1}H NMR and LC-UV-MS (Pinto et al., 2020). The phenolic compounds quantified were ellagic acid (1.23 mg/g DW), epigallocatechin (0.44 mg/g DW), catechin/epicatechin (0.32 mg/g DW), and a caffeic acid derivative (0.31 mg/g DW). Apigenin-7-*O*-rutinoside and luteolin-7-*O*-rutinoside were only identified. Nonetheless, a more exhaustive analysis was accomplished in this study to explore the untargeted metabolomic profiling. Table 1 presents the phenolic compounds quantified in the CSs extract.

According to Table 1, 6 phenolic compounds were quantified in the CSs extract, with a total content of 18.52 µg/mg DW, including 5 phenolic acids and 1 hydrolysable tannin. Ellagic acid was the major polyphenol quantified (6.96 µg/mg DW), representing 37.6 % of the total phenolic content. Additionally, *o*-coumaric acid (5.63 µg/mg DW), *p*-coumaric acid (2.73 µg/mg DW), ferulic acid (1.24 µg/mg DW), *trans*-caffeic acid (1.04 µg/mg DW), and *trans*-cinnamic acid (0.92 µg/mg DW) represent, respectively, 30.4 %, 14.7 %, 6.7 %, 5.6 %, and 5.0 % of the total phenolic content. Noteworthy, other polyphenols were identified in the extract, including 4-hydroxybenzoic acid (HBA), benzoic acid,

protocatechuic acid, 2,5-dihydroxybenzaldehyde, vanillin, vanillyl alcohol, feruladehyde, phenylacetic acid (PAA), 3,4-dihydroxyphenylacetic acid (dHPAA), 3-phenyllactic acid, phloretin, catechol, dihydrocapsaicin, esculetin, kievitone, marindinin, olivetonide, scopoletin, shogaol, umbelliferone, and 4-vinylphenol (**Supplementary Table 2**). The results demonstrated that the employment of ethanol as co-solvent enhanced the affinity to polar molecules, improving the phenolics recovery yield and the SFE performance, which explains the extraction of more hydrophilic phenolics as described in previous reports for other matrixes (Pimentel-Moral et al., 2019; Pinto et al., 2020).

In conclusion, CSs extract revealed to be rich in phenolic compounds and lipids whose bioactivity and pro-healthy benefits have been extensively documented in the last decades (Cádiz Gurrea et al., 2019; Ference, Graham, Tokgozoglu, & Catapano, 2018; Lobo, Patil, Phatak, & Chandra, 2010; Pinto et al., 2021). Previous reports on CSs extracts prepared by conventional and other green techniques (i.e., microwave-assisted extraction, subcritical water extraction (SWE), and ultrasound-assisted extraction) described identical phytochemical composition, with prevalence of phenolic acids (caffeic acid and derivatives, gallic acid, and protocatechuic acid), flavonoids (catechin and derivatives, apigenin, luteolin, quercetin, and myricetin derivatives) and hydrolysable tannins (ellagic acid) (Lameirão et al., 2020; Pinto et al., 2020; Pinto et al., 2021; Pinto et al., 2021; Rodrigues et al., 2015). The quantification of phenolic compounds in the CSs extract lays a primary foundation to investigate the permeation of phenolic compounds and metabolites across Caco-2/HT29-MTX intestinal barrier.

3.5. Permeation of phenolic compounds from CSs extract across intestinal barrier

Phenolic compounds and their metabolites undergo intestinal absorption after digestion (Pinto et al., 2023). Given the intricacy and dynamic nature of intestinal absorption, numerous *in-vitro* cellular models have emerged as exceptional approaches to simulate the human intestinal epithelium. These models have demonstrated high efficacy in the in-depth assessment of phenolics permeability across the intestinal barrier (Pinto et al., 2023). For the intestinal permeability assay, two CSs extract concentrations (100 and 1000 µg/mL) were tested on a Caco-2/HT29-MTX co-culture model. The concentrations were selected considering the findings of our previous study that sustained the *in-vitro* bioactivity and safety of CSs extract prepared by SFE in the two intestinal cells used for the intestinal permeability assay (Pinto et al., 2020). Table 2 summarizes the permeation rates of the CSs extract phenolic compounds and their metabolites (100 and 1000 µg/mL) at different times.

The main phenolic compounds that permeated across the intestinal barrier were HCAs and their metabolites, along with 1 hydrolysable tannin, 8 HBAs, 11 flavonoids, 4 coumarins, 2 HPAAs, and 1 HPPA. Nevertheless, it was only possible to quantify ellagic acid and HCAs. Dihydrocaffeic acid (DHCA), ferulic acid, dihydroferulic acid (DHFA), feruladehyde, *o*-coumaric acid, *p*-coumaric acid, and ellagic acid were quantified in the permeates of both extract concentrations tested, while *trans*-caffeic acid, hydroxyferulic acid, and *trans*-cinnamic acid were only quantified in the permeates from the CSs extract at 1000 µg/mL.

Considering the CSs extract at 100 µg/mL, the phenolics permeation enhanced in the following order: ellagic acid < *o*-coumaric acid < feruladehyde = DHFA ≤ *p*-coumaric acid < ferulic acid < DHCA, with increasing rates from 15 to 240 min. DHCA achieved the maximum intestinal permeability of 35.42 % at 240 min, followed by ferulic acid (28.12 % at 240 min). *p*-Coumaric acid (5.31–13.49 % from 15 to 240 min, respectively) permeated more efficiently the intestinal barrier than *o*-coumaric acid (2.60–7.15 %). DHFA and feruladehyde were only quantified at 180 and 240 min, achieving 12 % and 13 % permeation, respectively. Ellagic acid reached low permeation rates, with 2.51 and 2.99 %, respectively, at 15 and 240 min.

Regarding the CSs extract at 1000 µg/mL, the phenolics permeation

Table 1

Quantification of phenolic compounds in CSs extract prepared by SFE (*n* = 3).

Compound	Retention time (min)	$[M{-}H]^-$	Concentration (µg/mg DW) [a]
p-coumaric acid	7.065	163.0395	2.73 ± 0.03
Ferulic acid	9.717	193.0497	1.24 ± 0.10
trans-caffeic acid	10.055	179.0341	1.04 ± 0.06
trans-cinnamic acid	10.455	147.0448	0.92 ± 0.03
o-coumaric acid	11.273	163.0395	5.63 ± 0.12
Ellagic acid	13.017	300.9992	6.96 ± 1.95

[a] Compounds quantified in the SFE extract at 1 mg/mL.

Table 2
Permeation of phenolic compounds and metabolites from CSs extract prepared by SFE across intestinal co-culture model at different times ($n = 3$).

Sample	Compound/Metabolite	Permeation (%)							
		Time (min)							
		15	30	45	60	90	120	180	240
SFE extract 100 µg/mL	Dihydrocaffeic acid	13.03 ± 1.40[e,1]	15.69 ± 1.98[e,1]	18.75 ± 2.55[d,e,1]	21.33 ± 2.90[c,d,e,1]	25.54 ± 3.18[b,c,d,1]	27.15 ± 3.20[b,c,2]	31.53 ± 3.58[a,b,2]	35.42 ± 3.99[a,2]
	Ferulic acid	11.51 ± 0.02[h,1]	13.11 ± 0.08[g,1]	14.85 ± 0.03[f,1]	16.89 ± 0.10[e,1]	19.14 ± 0.13[d,1]	21.81 ± 0.10[c,1]	24.76 ± 0.23[b,1]	28.12 ± 0.12[a,1]
	Dihydroferulic acid	n.i.	n.i.	n.i.	n.i.	n.i.	n.i.	11.63 ± 0.09[b,2]	13.17 ± 0.03[a,2]
	Ferulaldehyde	n.i.	n.i.	n.i.	n.i.	n.i.	n.i.	11.58 ± 0.08[b,2]	13.13 ± 0.04[a,2]
	o-coumaric acid	2.60 ± 0.13[g,2]	3.03 ± 0.14[g,2]	3.60 ± 0.13[f,2]	4.16 ± 0.24[e,2]	4.80 ± 0.13[d,2]	5.45 ± 0.16[c,2]	6.34 ± 0.22[b,2]	7.15 ± 0.26[a,2]
	p-coumaric acid	5.31 ± 0.01[h,2]	6.06 ± 0.06[g,2]	7.01 ± 0.05[f,2]	8.08 ± 0.14[e,2]	9.12 ± 0.21[d,2]	10.42 ± 0.11[c,2]	11.82 ± 0.24[b,2]	13.49 ± 0.40[a,2]
	Ellagic acid	2.51 ± 0.74[a,b]	2.00 ± 0.41[a,b,1]	2.01 ± 0.38[a,b,1]	1.71 ± 0.60[b,2]	1.63 ± 0.27[b,2]	2.09 ± 0.21[a,b,2]	2.33 ± 0.55[a,b,2]	2.99 ± 0.64[a,2]
SFE extract 1000 µg/mL	*trans*-caffeic acid	13.55 ± 0.10[h]	15.28 ± 0.03[g]	17.38 ± 0.07[f]	19.69 ± 0.05[e]	22.33 ± 0.04[d]	25.31 ± 0.03[c]	28.82 ± 0.16[b]	32.62 ± 0.10[a]
	Dihydrocaffeic acid	13.38 ± 0.91[g,1]	16.83 ± 1.34[f,1]	19.81 ± 1.67[e,f,1]	23.21 ± 1.46[e,1]	28.61 ± 1.47[d,1]	32.67 ± 1.20[c,1]	37.72 ± 2.26[b,1]	44.61 ± 0.97[a,1]
	Ferulic acid	11.58 ± 0.14[f,1]	13.89 ± 0.70[e,1]	15.54 ± 0.88[e,1]	17.95 ± 1.19[d,1]	19.39 ± 0.30[d,2]	21.99 ± 0.34[c,1]	25.41 ± 0.94[b,1]	28.37 ± 0.47[a,1]
	Dihydroferulic acid	n.i.	11.75 ± 0.33[g]	13.49 ± 0.34[f]	15.79 ± 0.29[e]	17.91 ± 0.22[d]	20.40 ± 0.46[c]	23.70 ± 0.59[b,1]	26.95 ± 0.69[a,1]
	Hydroxyferulic acid	n.i.	11.94 ± 0.36[g]	13.63 ± 0.30[f]	15.52 ± 0.52[e]	17.91 ± 0.36[d]	20.29 ± 0.77[c]	23.33 ± 0.56[b]	26.52 ± 0.60[a]
	Ferulaldehyde	n.i.	11.75 ± 0.17[g]	13.42 ± 0.12[f]	15.31 ± 0.20[e]	17.50 ± 0.19[d]	20.17 ± 0.20[c]	22.67 ± 0.52[b,1]	25.94 ± 0.66[a,1]
	trans-cinnamic acid	14.46 ± 0.31[h]	16.96 ± 0.30[g]	19.31 ± 0.37[f]	22.28 ± 0.42[e]	25.60 ± 0.62[d]	29.47 ± 0.83[c]	33.45 ± 1.23[b]	38.49 ± 1.30[a]
	o-coumaric acid	2.82 ± 0.06[f,1]	4.59 ± 0.27[d,e,f,1]	5.43 ± 0.41[c,e,1]	6.80 ± 0.29[c,d,1]	7.63 ± 0.58[c,1]	9.71 ± 0.54[b,c,1]	11.95 ± 1.02[a,b,1]	12.79 ± 1.76[a,1]
	p-coumaric acid	5.70 ± 0.25[g,1]	7.43 ± 0.56[f,g,1]	8.58 ± 0.72[e,f,1]	10.33 ± 0.78[e,1]	13.05 ± 0.62[d,1]	15.66 ± 0.58[c,1]	18.51 ± 1.26[b,1]	20.90 ± 2.17[a,1]
	Ellagic acid	n.d.	1.82 ± 0.45[d,1]	1.99 ± 0.10[d,1]	3.51 ± 0.75[b,c,1]	4.42 ± 0.32[a,c,1]	5.95 ± 1.42[a,b,1]	9.39 ± 1.34[a,1]	9.55 ± 2.04[a,1]

n.i., not identified. n.d., not determined. Different letters (a–h) indicate significant differences ($p < 0.05$) between permeation times. Different numbers (1 and 2) indicate significant differences ($p < 0.05$) between extract concentrations.

improved as follows: ellagic acid < *o*-coumaric acid < *p*-coumaric acid < ferulaldehyde ≤ hydroxyferulic acid ≤ DHFA < ferulic acid < *trans*-caffeic acid < *trans*-cinnamic acid < DHCA. The permeation rates also steadily increased from 15 to 240 min. DHCA reached the highest intestinal permeability, varying between 13.38 % and 44.61 %, respectively, at 15 and 240 min. Almost 40 % of *trans*-cinnamic acid and 33 % of *trans*-caffeic acid permeated after 240 min, being only quantified for the highest extract concentration tested. The intestinal permeation of ferulic acid, DHFA, hydroxyferulic acid, and ferulaldehyde was above 25 % after 4 h. Additionally, *o*-coumaric and *p*-coumaric acids achieved, respectively, 13 % and 21 % of maximum permeation. As attested for 100 µg/mL CSs extract, ellagic acid had the lowest permeation rates, attaining only 10 % at 240 min, which may be due to its biotransformation into metabolites and low solubility in aqueous solvents, influencing its intestinal permeation (Pinto et al., 2023). In general, significant differences ($p < 0.05$) were noticed between the two extract concentrations tested for DHCA, DHFA, ferulaldehyde, *o*-coumaric acid, *p*-coumaric acid, and ellagic acid. Only similar permeation rates ($p > 0.05$) were determined for ferulic acid. Furthermore, a considerable fraction of phenolic compounds with poor intestinal permeability may be probably retained in the intestinal barrier owing to their complex chemical structures and biotransformation into metabolites difficult to detect (considering the absence of standards and interferences with cellular constituents), hindering their passage from the apical to the basolateral side. These phenolics retained in the cell barrier may also exert pro-healthy benefits (such as cell cytoprotection), mitigating the oxidative stress consequences implicated in the transport of phenolic compounds through cell membranes.

The P_{app} coefficient was determined as an accurate indicator of the speed at which phenolic compounds permeate the intestinal membrane, offering insights into the mechanisms underlying their intestinal absorption (Araújo & Sarmento, 2013; Pinto et al., 2023). Fig. 3 presents the TEER values during the permeation assay and the P_{app} coefficients calculated at 240 min.

As shown in Fig. 3C, the P_{app} values are in line with the permeation rates presented in Table 2. The highest permeation rates were obtained for DHCA (10.98×10^{-6} and 13.83×10^{-6} cm/s, respectively, for 100 and 1000 µg/mL CSs extract) and *trans*-cinnamic acid (11.93×10^{-6} cm/s for 1000 µg/mL). Similar P_{app} values were determined for ferulic acid, hydroxyferulic acid and ferulaldehyde ($\approx 8 \times 10^{-6}$ cm/s), while DHFA reached around 4×10^{-6} cm/s. Higher P_{app} values were determined for *p*-coumaric acid (4.18×10^{-6} and 6.48×10^{-6} cm/s, respectively) than *o*-coumaric acid (2.22×10^{-6} and 3.97×10^{-6} cm/s). The lowest P_{app} values were achieved for ellagic acid with 0.93×10^{-6} and 2.96×10^{-6} cm/s, respectively, for 100 and 1000 µg/mL. Recently, Rocchetti et al. (2024) proved effective permeation of anthocyanins, flavones, flavanols, flavonols, phenolic acids, and stilbenes across Caco-2 monolayers, highlighting better P_{app} coefficients for phenolic acids ($1.16–1.95 \times 10^{-4}$ cm/s), flavones ($0.61–1.32 \times 10^{-4}$ cm/s) and anthocyanins ($0.39–1.78 \times 10^{-4}$ cm/s). The P_{app} values are also identical to those determined by Henriques, Falé, Pacheco, Florêncio, and Serralheiro (2018) for rutin (8.1×10^{-6} cm/s) and quercitrin (7.6×10^{-6} cm/s) from *Actinidia deliciosa* leaves through Caco-2 monolayers. Overall, the P_{app} values sustained a considerably high permeation of phenolic compounds across the intestinal barrier (except for ellagic acid from 100 µg/mL extract) considering the results higher than 1×10^{-6} cm/s,

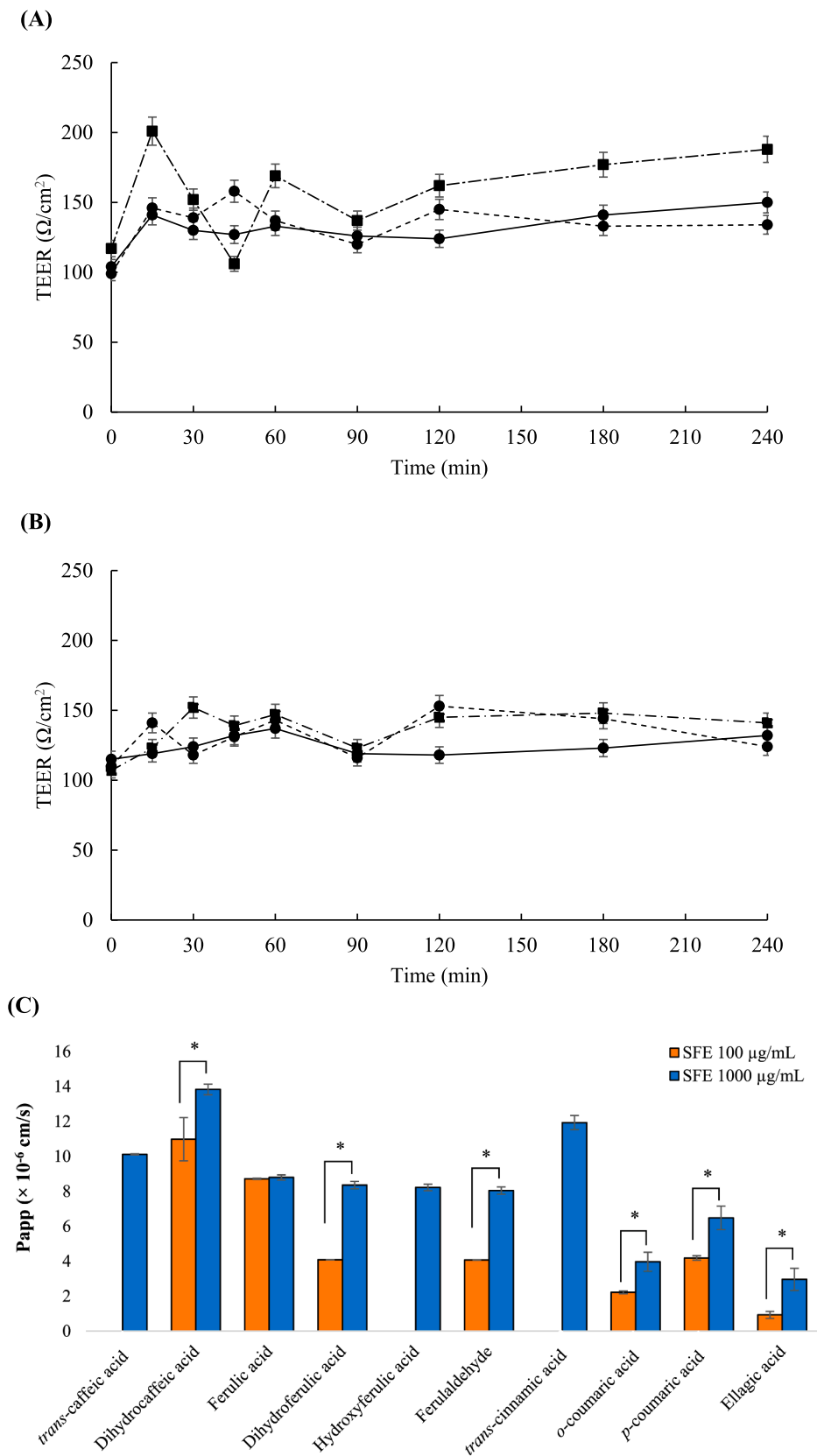**(A)**

(B)

(C)

Fig. 3. Transepithelial electrical resistance (TEER) and coefficient of permeability (P_{app}) measured during the intestinal permeability assay ($n = 3$). (A) TEER values in SFE extract at 100 μg/mL, (B) TEER values in SFE extract at 1000 μg/mL, (C) P_{app} values at 240 min. * denotes significant differences ($p < 0.05$) between extract concentrations.

enabling them to reach the target site and exert the therapeutic effects, mainly oxidative protection.

The TEER was monitored during the experiment to ensure the integrity of cells barrier (Pinto et al., 2023). For 100 μg/mL CS extract, the TEER values varied between 99 Ω/cm² (15 min) and 188 Ω/cm² (240 min), maintaining stable since 120 min (Fig. 3A). Considering the 1000 μg/mL extract, the TEER values reached 107 Ω/cm² (15 min) and 141 Ω/cm² (240 min), remaining constant from 120 to 240 min (Fig. 3B). These values are in line with the ones reported by Pinto, Silva, Dall'Acqua et al. (2023) to evaluate the intestinal permeation of CSs extract prepared by SWE across a similar *in-vitro* model (135–171 Ω/cm²). Nonetheless, higher TEER values were reported for Caco-2 monocultures (≤400 Ω/cm²), Caco-2/Raji B co-cultures (≤250 Ω/cm²), and Caco-2/HT29-MTX/Raji B triple culture (≤225 Ω/cm²) (Araújo & Sarmento, 2013) possibly due to the action of mucus-secreting HT29-MTX cells that regulate the Caco-2 tight junctions, enhancing the intercellular spaces among Caco-2 and HT29-MTX cells and, consequently, affecting the transport of phenolics through the intestinal barrier (Araújo & Sarmento, 2013).

Given the promising therapeutic effects of phenolic compounds, an in-depth assessment of their intestinal absorption is vital to comprehend the *in-vivo* bioactivity. Recent studies have reported identical findings using intestinal cell models (Grzelczyk et al., 2022; Pinto et al., 2023; Prado Massarioli et al., 2023). Grzelczyk et al. (2022) described the uptake of caffeic and ferulic acids from coffee beans extracts across Caco-2 monolayers. Prado Massarioli et al. (2023) demonstrated the permeation of *p*-coumaric acid and derivatives from peanuts digest above 10 % after 4 h. For instance, a previous study from our research team demonstrated the intestinal absorption of ellagic acid from a CSs extract prepared by SWE, with 23 % of permeation after 4 h using the same intestinal co-culture model (Pinto et al., 2023). These reports corroborate the outcomes of the present study, emphasizing the effective permeation of HCAs metabolites and ellagic acid across intestinal models (Grzelczyk et al., 2022; Pinto et al., 2023; Prado Massarioli et al., 2023; Rocchetti et al., 2024).

3.6. Possible metabolic pathways of phenolic compounds upon intestinal permeation

The physiological importance of phenolic compounds relies on their bioavailability for intestinal absorption that is directly influenced by metabolic pathways (Pinto et al., 2023; Rocchetti et al., 2024). In this

Fig. 4. Metabolic pathways proposed for the phenolic compounds and metabolites permeated across the intestinal barrier.

work, a Caco-2/HT29-MTX model was used to mimic the enterocytes, described as an important site for HCAs metabolism. Noteworthy, this is the first study that explores the metabolomic profiling of phenolic-rich CSs extract prepared by SFE upon *in-vitro* intestinal permeation. Fig. 4 represents the main metabolic pathways of the phenolic compounds permeated across the intestinal barrier.

Most of the metabolites identified in the permeates resulted from phase I metabolism (i.e., hydrolysis, reduction, oxidation, hydrogenation), while a minor fraction arisen from phase II reactions (methylation). As depicted in Fig. 4, caffeic and ferulic acids may be biotransformed into their reduced metabolites via hydrogenation, forming DHCA and DHFA that can be absorbed through intestinal epithelium, corroborating their considerable permeation rates across Caco-2/HT29-MTX model (Pinto et al., 2023; Pinto et al., 2023; Sova & Saso, 2020). Concerning DHCA, 3-HPPA and 3,4-dHPAA are the direct products that are dehydroxylated to 3-HPAA (Pinto et al., 2023; Sadeghi Ekbatan et al., 2018; Sova & Saso, 2020). Additionally, the removal of methoxy group from DHFA originates 4-HPPA, further metabolized by two pathways: i) dehydroxylation into 3-PPA that may be bioconverted into PAA and benzoic acid; or ii) hydrolysis into 4-HPAA and, subsequently, 4-HBA (Pinto et al., 2023; Sadeghi Ekbatan et al., 2018; Sova & Saso, 2020). Alternatively, caffeic acid may be dehydroxylated into coumaric acid and further cinnamic acid, which originates 4-HBA and benzoic acid by loss of carbons and dehydroxylation (Pinto et al., 2023; Sadeghi Ekbatan et al., 2018; Sova & Saso, 2020). Caffeic acid may be also a precursor of ferulic acid via methylation, while ferulic acid is a precursor of ferulaldehyde (reduction) and hydroxyferulic acid (hydroxylation) (Pinto et al., 2023; Radnai et al., 2009). In addition, ferulic acid may be biotransformed into vanillic acid that may originate protocatechuic acid by demethylation and, subsequently, catechol by decarboxylation (Pinto et al., 2023; Sova & Saso, 2020). Vanillic acid may be also metabolized by two other pathways: i) reduction and formation of vanillin and vanillyl alcohol; and ii) decarboxylation producing guaiacol (Alvarez-Rodríguez et al., 2003). Furthermore, cinnamic and *p*-coumaric acids may be synthetized from amino acids, respectively, from phenylalanine and tyrosine (Cui et al., 2020). These metabolic pathways were proposed by Sadeghi Ekbatan et al. (2018) that reported up to 15 % of permeation of ferulic acid, DHCA and DHFA, and up to 5 % of 3-HBA, 3-HPPA, and coumaric acid from potato extract digest through a Caco-2/HepG2 co-culture model. Konishi and Kobayashi (2004) demonstrated that HPPA, dHPPA, and *m*-coumaric acid are the main caffeic and chlorogenic acids metabolites upon Caco-2 monolayers permeation.

Regarding flavanones, naringenin undergoes different metabolic pathways including: i) methylation (producing naringenin dimethyl ether); ii) dehydrogenation into apigenin and subsequent methylation (dimethyl-apigenin) or hydroxylation (luteolin); iii) formation of *p*-coumaric acid by ring fission and further hydroxylation (caffeic acid), dehydroxylation (cinnamic acid), and hydrogenation (3-HPPA); or iv) C-ring cleavage into phloretin (Zeng et al., 2022). Luteolin may undergo methylation (luteolin dimethyl ether), hydroxylation plus methylation (hydroxyluteolin methyl ether), and methoxylation plus methylation (methoxyluteolin methyl ether) (Wang et al., 2017), while phloretin may be hydrolyzed into phloroglucinol and 3-HPPA (Orrego-Lagarón, Martínez-Huélamo, Vallverdú-Queralt, Lamuela-Raventos, & Escribano-Ferrer, 2015). Tian, Yang, Yang, and Wang (2009) investigated the intestinal permeability of 36 flavonoids, achieving 18 %, 21 %, and 15 % of permeation, respectively, for apigenin, luteolin, and naringenin across a Caco-2 monolayer.

Considering coumarins, the main pathways encompass 7-hydroxylation (forming 7-hydroxycoumarin) and 3,4-epoxidation (obtaining HPAA as final product) (Hsieh et al., 2019). Moreover, *o*-coumaric acid is also a possible metabolite formed by ring fission (Hsieh et al., 2019). Scopoletin may be formed from ferulic acid via *trans/cis* spontaneous isomerization and lactonization, while umbelliferone results from hydroxylation and *trans/cis* isomerization and lactonization of coumaric acid (Srinivasa et al., 2022). Alternatively, umbelliferone may be hydroxylated into esculetin and then methoxylated into scopoletin (Hijazin, Radwan, Abouzeid, Dräger, & Selmar, 2019). These pathways may explain the presence of scopoletin, umbelliferone, and esculetin in CSs extract and permeates. Galkin, Fallarero, and Vuorela (2009) studied the coumarins permeability, identifying scopoletin and umbelliferone in the permeates, along with hydroxylated, methylated and methoxylated conjugates.

Other metabolites identified were 3-phenyllactic acid and dihydrocapsaicin. 3-Phenyllactic acid is involved in the phenylalanine metabolism. Phenylalanine is metabolized via transamination into PAA, phenylpyruvate and phenethylamine (Tekewe, Singh, Singh, Mohan, & Banerjee, 2008). 3-Phenyllactic acid is then produced from phenylpyruvate by lactate dehydrogenase (Tekewe et al., 2008). Dihydrocapsaicin may result from the hydrogenation of capsaicin and bioconversion into vanillin, vanillic acid and vanillyl alcohol by enzymatic hydrolysis (Noami et al., 2006). In conclusion, HBAs, HPAAs, and HPPAs are the principal metabolites of more complex phenolic compounds, mainly HCAs and flavonoids. Among HCAs metabolites, it highlights 4-HBA, benzoic acid, vanillin, vanillyl alcohol, and protocatechuic acid, while the main HPAAs and HPPAs are PAA, 3,4-dHPAA, and 3-phenyllactic acid. In addition, 2,5-dihydroxybenzaldehyde can be formed by reduction of 2,5-dihydroxybenzoic acid.

4. Conclusion

The intestinal permeability of phenolic-rich CSs extract prepared by SFE was investigated using an intestinal co-culture model by combining with metabolomics. The extract showed mild to strong inhibitory responses on AChE, α-amylase, and lipase activities, probably ascribed to the phenolic composition, namely ellagic, *o*-coumaric, *p*-coumaric, ferulic, *trans*-caffeic, and *trans*-cinnamic acids. The untargeted metabolic profile of the extract and permeates revealed that lipids and phenolic compounds represent almost 90 % of the annotated compounds, with 29 metabolic pathways indicated by KEGG enrichment analysis. Among phenolics, caffeic and ferulic acids and their reduced conjugates were the main phenolic metabolites permeating the intestinal barrier, along with hydroxyferulic acid, ferulaldehyde, *p*-coumaric acid, *o*-coumaric acid, *trans*-cinnamic acid and ellagic acid. Apigenin and luteolin metabolites were also identified in permeates arising from methylation, hydroxylation and methoxylation. The results pointed out pronounced differences in the intestinal permeability profiles of phenolic compounds for different extract concentrations (100 and 1000 μg/mL) and time-points (15–240 min). The annotated compounds (mainly phenolics) may act as functional markers of oxidative protection and enzymatic bioactivity on AChE, α-amylase, and lipase, proving the intestinal absorption of phenolics-rich CSs extract and sustaining a possible final application as nutraceutical ingredient with interesting pro-healthy benefits.

CRediT authorship contribution statement

Diana Pinto: Methodology, Software, Formal analysis, Investigation, Writing – original draft. **Julián Lózano-Castellón:** Methodology, Formal analysis, Investigation, Writing – review & editing. **Ana Margarida Silva:** Methodology, Formal analysis, Investigation. **María de la Luz Cádiz-Gurrea:** Methodology, Formal analysis, Investigation. **Antonio Segura-Carretero:** Funding acquisition, Resources. **Rosa Lamuela-Raventós:** Methodology, Funding acquisition, Resources. **Anna Vallverdú-Queralt:** Methodology, Supervision, Writing – review & editing. **Cristina Delerue-Matos:** Methodology, Supervision, Resources. **Francisca Rodrigues:** Methodology, Conceptualization, Validation, Investigation, Resources, Writing – review & editing, Supervision, Project administration, Funding acquisition.

Declaration of Competing Interest

The authors declare that they have no known competing financial interests or personal relationships that could have appeared to influence the work reported in this paper.

Data availability

The authors do not have permission to share data.

Appendix A. Supplementary material

Supplementary data to this article can be found online at https://doi.org/10.1016/j.foodres.2023.113807.

References

Aloo, S.-O., Ofosu, F. K., Kim, N.-H., Kilonzi, S. M., & Oh, D.-H. (2023). Insights on dietary polyphenols as agents against metabolic disorders: Obesity as a target disease. *Antioxidants, 12*(2), 416. https://doi.org/10.3390/antiox12020416

Alvarez-Rodríguez, M., Belloch, C., Villa, M., Uruburu, F., Larriba, G., & Coque, J. J. R. (2003). Degradation of vanillic acid and production of guaiacol by microorganisms isolated from cork samples. *FEMS Microbiology Letters, 220*(1), 49–55. https://doi.org/10.1016/S0378-1097(03)00053-3

Araújo, F., & Sarmento, B. (2013). Towards the characterization of an *in vitro* triple co-culture intestine cell model for permeability studies. *International Journal of Pharmaceutics, 458*(1), 128–134. https://doi.org/10.1016/j.ijpharm.2013.10.003

Cádiz Gurrea, M.d.l. L., Soares, S., Jiménez, F. J. L., Ochoa, Á. F., Pinto, D., Delerue-Matos, C., … Rodrigues, F. (2019). Chapter 4 - Effects of nutritional supplements on human health. In C. M. Galanakis (Ed.), *Nutraceuticals and Natural Product Pharmaceuticals* (pp. 105–140). Academic Press. https://doi.org/10.1016/B978-0-12-816450-1.00004-0.

Crozier, A., Del Rio, D., & Clifford, M. N. (2010). Bioavailability of dietary flavonoids and phenolic compounds. *Molecular Aspects of Medicine, 31*(6), 446–467. https://doi.org/10.1016/j.mam.2010.09.007

Cui, P., Zhong, W., Qin, Y., Tao, F., Wang, W., & Zhan, J. (2020). Characterization of two new aromatic amino acid lyases from actinomycetes for highly efficient production of *p*-coumaric acid. *Bioprocess and Biosystems Engineering, 43*(7), 1287–1298. https://doi.org/10.1007/s00449-020-02325-5

de Francisco, L. M. B., Pinto, D., Rosseto, H. C., de Toledo, L.d. A. S., Dos Santos, R. S., Costa, P. C., … Bruschi, M. L. (2018). Development of a microparticulate system containing Brazilian propolis by-product and gelatine for ascorbic acid delivery: Evaluation of intestinal cell viability and radical scavenging activity. *Food & Function, 9*(8), 4194–4206. https://doi.org/10.1039/C8FO00863A

Escobar-Avello, D., Mardones, C., Saéz, V., Riquelme, S., von Baer, D., Lamuela-Raventós, R. M., & Vallverdú-Queralt, A. (2021). Pilot-plant scale extraction of phenolic compounds from grape canes: Comprehensive characterization by LC-ESI-LTQ-Orbitrap-MS. *Food Research International, 143*, Article 110265. https://doi.org/10.1016/j.foodres.2021.110265

Fatima, M. T., Bhat, A. A., Nisar, S., Fakhro, K. A., & Al-Shabeeb Akil, A. S. (2023). The role of dietary antioxidants in type 2 diabetes and neurodegenerative disorders: An assessment of the benefit profile. *Heliyon, 9*(1), e12698.

Ference, B. A., Graham, I., Tokgozoglu, L., & Catapano, A. L. (2018). Impact of lipids on cardiovascular health: JACC Health Promotion Series. *Journal of the American College of Cardiology, 72*(10), 1141–1156. https://doi.org/10.1016/j.jacc.2018.06.046

Fernández-Ochoa, Á., Cádiz-Gurrea, M.d.l. L., Fernández-Moreno, P., Rojas-García, A., Arráez-Román, D., & Segura-Carretero, A. (2022). Recent analytical approaches for the study of bioavailability and metabolism of bioactive phenolic compounds. *Molecules, 27*(3), 777. https://doi.org/10.3390/molecules27030777

Galkin, A., Fallarero, A., & Vuorela, P. M. (2009). Coumarins permeability in Caco-2 cell model. *Journal of Pharmacy and Pharmacology, 61*(2), 177–184. https://doi.org/10.1211/jpp.61.02.0006

Gamboa-Gómez, C. I., Simental-Mendía, L. E., González-Laredo, R. F., Alcantar-Orozco, E. J., Monserrat-Juarez, V. H., Ramírez-España, J. C., … Rocha-Guzmán, N. E. (2017). *In vitro* and *in vivo* assessment of anti-hyperglycemic and antioxidant effects of Oak leaves (*Quercus convallata* and *Quercus arizonica*) infusions and fermented beverages. *Food Research International, 102*, 690–699. https://doi.org/10.1016/j.foodres.2017.09.040

González, F., García-Martínez, E., Del Mar Camacho, M., Martínez-Navarrete, N., Sarmento, B., Fernandes, I., … Oliveira, B. (2019). Insights into the development of grapefruit nutraceutical powder by spray drying: Physical characterization, chemical composition and 3D intestinal permeability. *Journal of the Science of Food and Agriculture, 99*(10), 4686–4694. https://doi.org/10.1002/jsfa.9709

Grzelczyk, J., Szwajgier, D., Baranowska-Wójcik, E., Budryn, G., Zakłos-Szyda, M., & Sosnowska, B. (2022). Bioaccessibility of coffee bean hydroxycinnamic acids during *in vitro* digestion influenced by the degree of roasting and activity of intestinal probiotic bacteria, and their activity in Caco-2 and HT29 cells. *Food Chemistry, 392*, Article 133328. https://doi.org/10.1016/j.foodchem.2022.133328

Henriques, J., Falé, P. L., Pacheco, R., Florêncio, M. H., & Serralheiro, M. L. (2018). Phenolic compounds from *Actinidia deliciosa* leaves: Caco-2 permeability, enzyme inhibitory activity and cell protein profile studies. *Journal of King Saud University - Science, 30*(4), 513–518. https://doi.org/10.1016/j.jksus.2017.07.007

Herrera-Balandrano, D. D., Wang, J., Chai, Z., Zhang, X., Wang, N., & Huang, W. (2023). Impact of *in vitro* gastrointestinal digestion on rabbiteye blueberry anthocyanins and their absorption efficiency in Caco-2 cells. *Food Bioscience, 52*, Article 102424. https://doi.org/10.1016/j.fbio.2023.102424

Hijazin, T., Radwan, A., Abouzeid, S., Dräger, G., & Selmar, D. (2019). Uptake and modification of umbelliferone by various seedlings. *Phytochemistry, 157*, 194–199. https://doi.org/10.1016/j.phytochem.2018.10.032

Hsieh, C. J., Sun, M., Osborne, G., Ricker, K., Tsai, F. C., Li, K., … Sandy, M. S. (2019). Cancer hazard identification integrating human variability: The case of coumarin. *International Journal of Toxicology, 38*(6), 501–552. https://doi.org/10.1177/1091581819884544

Hu, Y., Lin, Q., Zhao, H., Li, X., Sang, S., McClements, D. J., … Qiu, C. (2023). Bioaccessibility and bioavailability of phytochemicals: Influencing factors, improvements, and evaluations. *Food Hydrocolloids, 135*, Article 108165. https://doi.org/10.1016/j.foodhyd.2022.108165

Konishi, Y., & Kobayashi, S. (2004). Microbial metabolites of ingested caffeic acid are absorbed by the monocarboxylic acid transporter (MCT) in intestinal Caco-2 cell monolayers. *Journal of Agricultural and Food Chemistry, 52*(21), 6418–6424. https://doi.org/10.1021/jf049560y

Lameirão, F., Pinto, D., Vieira, E. F., Peixoto, A., Freire, C., Sut, S., … Rodrigues, F. (2020). Green-sustainable recovery of phenolic and antioxidant compounds from industrial chestnut shells using ultrasound-assisted extraction: Optimization and evaluation of biological activities *in vitro*. *Antioxidants, 9*(3), 267. https://doi.org/10.3390/antiox9030267

Laveriano-Santos, E. P., Marhuenda-Muñoz, M., Vallverdú-Queralt, A., Martínez-Huélamo, M., Tresserra-Rimbau, A., Miliarakis, E., … Lamuela-Raventós, R. M. (2022). Identification and quantification of urinary microbial phenolic metabolites by HPLC-ESI-LTQ-Orbitrap-HRMS and their relationship with dietary polyphenols in adolescents. *Antioxidants, 11*(6), 1167. https://doi.org/10.3390/antiox11061167

Lobo, V., Patil, A., Phatak, A., & Chandra, N. (2010). Free radicals, antioxidants and functional foods: Impact on human health. *Pharmacognosy Reviews, 4*(8), 118–126. https://doi.org/10.4103/0973-7847.70902

Lozano-Castellón, J., Rocchetti, G., Vallverdú-Queralt, A., Lucchini, F., Giuberti, G., Torrado-Prat, X., … Lucini, L. (2022). New insights into the lipidomic response of Caco-2 cells to differently cooked and *in vitro* digested extra-virgin olive oils. *Food Research International, 155*, Article 111030. https://doi.org/10.1016/j.foodres.2022.111030

Martinelli, E., Granato, D., Azevedo, L., Gonçalves, J. E., Lorenzo, J. M., Munekata, P. E. S., … Lucini, L. (2021). Current perspectives in cell-based approaches towards the definition of the antioxidant activity in food. *Trends in Food Science & Technology, 116*, 232–243. https://doi.org/10.1016/j.tifs.2021.07.024

Martins, N., Barros, L., & Ferreira, I. C. F. R. (2016). *In vivo* antioxidant activity of phenolic compounds: Facts and gaps. *Trends in Food Science & Technology, 48*, 1–12. https://doi.org/10.1016/j.tifs.2015.11.008

Neves, J. M., Matos, C., Moutinho, C., Queiroz, G., & Gomes, L. R. (2009). Ethnopharmacological notes about ancient uses of medicinal plants in Trás-os-Montes (northern of Portugal). *Journal of Ethnopharmacology, 124*(2), 270–283. https://doi.org/10.1016/j.jep.2009.04.041

Noami, M., Igarashi, K., Kasuya, F., Ohta, M., Kanamori-Kataoka, M., & Seto, Y. (2006). Study on the analysis of capsaicin glucuronide in rat urine by liquid chromatography-mass spectrometry after enzymatic hydrolysis. *Journal of Health Science, 52*(6), 660–665. https://doi.org/10.1248/jhs.52.660

Orrego-Lagarón, N., Martínez-Huélamo, M., Vallverdú-Queralt, A., Lamuela-Raventos, R. M., & Escribano-Ferrer, E. (2015). High gastrointestinal permeability and local metabolism of naringenin: Influence of antibiotic treatment on absorption

and metabolism. *British Journal of Nutrition, 114*(2), 169–180. https://doi.org/10.1017/S0007114515001671

Pan, Y., Li, H., Shahidi, F., Luo, T., & Deng, Z. (2022). Interactions among dietary phytochemicals and nutrients: Role of cell membranes. *Trends in Food Science & Technology, 124*, 38–50. https://doi.org/10.1016/j.tifs.2022.03.024

Pérez, A. J., Pecio, Ł., Kowalczyk, M., Kontek, R., Gajek, G., Stopinsek, L., … Oleszek, W. (2017). Cytotoxic triterpenoids isolated from sweet chestnut heartwood (*Castanea sativa*) and their health benefits implication. *Food and Chemical Toxicology, 109*, 863–870. https://doi.org/10.1016/j.fct.2017.03.049

Pimentel-Moral, S., Borrás-Linares, I., Lozano-Sánchez, J., Arráez-Román, D., Martínez-Férez, A., & Segura-Carretero, A. (2019). Supercritical CO$_2$ extraction of bioactive compounds from *Hibiscus sabdariffa*. *The Journal of Supercritical Fluids, 147*, 213–221. https://doi.org/10.1016/j.supflu.2018.11.005

Pinto, D., Almeida, A., López-Yerena, A., Pinto, S., Sarmento, B., Lamuela-Raventós, R., … Rodrigues, F. (2023). Appraisal of a new potential antioxidants-rich nutraceutical ingredient from chestnut shells through *in-vivo* assays – A targeted metabolomic approach in phenolic compounds. *Food Chemistry, 404*, Article 134546. https://doi.org/10.1016/j.foodchem.2022.134546

Pinto, D., Braga, N., Silva, A. M., Costa, P., Delerue-Matos, C., & Rodrigues, F. (2020). Chapter 6 - Chestnut. In C. M. Galanakis (Ed.), *Valorization of Fruit Processing By-products* (pp. 127–144). Academic Press. https://doi.org/10.1016/j.foodchem.2022.134546.

Pinto, D., Cádiz-Gurrea, M.d.l. L., Garcia, J., Saavedra, M. J., Freitas, V., Costa, P., … Rodrigues, F. (2021). From soil to cosmetic industry: Validation of a new cosmetic ingredient extracted from chestnut shells. *Sustainable Materials and Technologies, 29*, e00309.

Pinto, D., Cádiz-Gurrea, M.d.l. L., Sut, S., Ferreira, A. S., Leyva-Jimenez, F. J., Dall'Acqua, S., … Rodrigues, F. (2020). Valorisation of underexploited *Castanea sativa* shells bioactive compounds recovered by supercritical fluid extraction with CO$_2$: A response surface methodology approach. *Journal of CO2 Utilization, 40*, Article 101194. https://doi.org/10.1016/j.jcou.2020.101194

Pinto, D., Cádiz-Gurrea, M.d.l. L., Vallverdú-Queralt, A., Delerue-Matos, C., & Rodrigues, F. (2021). *Castanea sativa* shells: A review on phytochemical composition, bioactivity and waste management approaches for industrial valorization. *Food Research International, 144*, Article 110364. https://doi.org/10.1016/j.foodres.2021.110364

Pinto, D., Delerue-Matos, C., & Rodrigues, F. (2020). Bioactivity, phytochemical profile and pro-healthy properties of *Actinidia arguta*: A review. *Food Research International, 136*, Article 109449. https://doi.org/10.1016/j.foodres.2020.109449

Pinto, D., Ferreira, A. S., Lozano-Castellón, J., Laveriano-Santos, E. P., Lamuela-Raventós, R. M., Vallverdú-Queralt, A., … Rodrigues, F. (2023). Exploring the impact of *in vitro* gastrointestinal digestion in the bioaccessibility of phenolic-rich chestnut shells: A preliminary study. *Separations, 10*(9), 471. https://doi.org/10.3390/separations10090471

Pinto, D., López-Yerena, A., Almeida, A., Sarmento, B., Lamuela-Raventós, R., Vallverdú-Queralt, A., … Rodrigues, F. (2023). Metabolomic insights into phenolics-rich chestnut shells extract as a nutraceutical ingredient – A comprehensive evaluation of its impacts on oxidative stress biomarkers by an *in-vivo* study. *Food Research International, 170*, Article 112963. https://doi.org/10.1016/j.foodres.2023.112963

Pinto, D., López-Yerena, A., Lamuela-Raventós, R., Vallverdú-Queralt, A., Delerue-Matos, C., & Rodrigues, F. (2024). Predicting the effects of *in-vitro* digestion in the bioactivity and bioaccessibility of antioxidant compounds extracted from chestnut shells by supercritical fluid extraction – A metabolomic approach. *Food Chemistry, 435*, Article 137581. https://doi.org/10.1016/j.foodchem.2023.137581

Pinto, D., Silva, A. M., Dall'Acqua, S., Sut, S., Vallverdú-Queralt, A., Delerue-Matos, C., & Rodrigues, F. (2023). Simulated gastrointestinal digestion of chestnut (*Castanea sativa* Mill.) shell extract prepared by subcritical water extraction: Bioaccessibility, bioactivity, and intestinal permeability by *in vitro* assays. *Antioxidants, 12*(7), 1414. https://doi.org/10.3390/antiox12071414

Pinto, D., Silva, A. M., Freitas, V., Vallverdú-Queralt, A., Delerue-Matos, C., & Rodrigues, F. (2021). Microwave-assisted extraction as a green technology approach to recover polyphenols from *Castanea sativa* shells. *ACS Food Science & Technology, 1*(2), 229–241. https://doi.org/10.1021/acsfoodscitech.0c00055

Pinto, D., Vieira, E. F., Peixoto, A. F., Freire, C., Freitas, V., Costa, P., … Rodrigues, F. (2021). Optimizing the extraction of phenolic antioxidants from chestnut shells by subcritical water extraction using response surface methodology. *Food Chemistry, 334*, Article 127521. https://doi.org/10.1016/j.foodchem.2020.127521

Prado Massarioli, A., de Oliveira, G., Sartori, A., Francetto Juliano, F., Gomes, E. P., do Amaral, J., … Matias de Alencar, S. (2023). Simulated gastrointestinal digestion/Caco-2 cell model to predict bioaccessibility and intestinal permeability of *p*-coumaric acid and *p*-coumaroyl derivatives in peanut. *Food Chemistry, 400*, Article 134033. https://doi.org/10.1016/j.foodchem.2022.134033

Radnai, B., Tucsek, Z., Bognar, Z., Antus, C., Mark, L., Berente, Z., … Veres, B. (2009). Ferulaldehyde, a water-soluble degradation product of polyphenols, inhibits the lipopolysaccharide-induced inflammatory response in mice. *The Journal of Nutrition, 139*(2), 291–297. https://doi.org/10.3945/jn.108.097386

Rocchetti, G., Lucini, L., Eduardo Gonçalves, J., Camps, I., dos Santos Lima, A., Granato, D., … Azevedo, L. (2024). Cellular assays combined with metabolomics highlight the dual face of phenolics: From high permeability to morphological cell damage. *Food Chemistry, 430*, Article 137081. https://doi.org/10.1016/j.foodchem.2023.137081

Rocchetti, G., Tomas, M., Zhang, L., Zengin, G., Lucini, L., & Capanoglu, E. (2020). Red beet (*Beta vulgaris*) and amaranth (*Amaranthus* sp.) microgreens: Effect of storage and *in vitro* gastrointestinal digestion on the untargeted metabolomic profile. *Food Chemistry, 332*, Article 127415. https://doi.org/10.1016/j.foodchem.2020.127415

Rodrigues, F., Santos, J., Pimentel, F. B., Braga, N., Palmeira-de-Oliveira, A., & Oliveira, M. B. (2015). Promising new applications of *Castanea sativa* shell: Nutritional composition, antioxidant activity, amino acids and vitamin E profile. *Food & Function, 6*(8), 2854–2860. https://doi.org/10.1039/c5fo00571j

Sadeghi Ekbatan, S., Iskandar, M. M., Sleno, L., Sabally, K., Khairallah, J., Prakash, S., & Kubow, S. (2018). Absorption and metabolism of phenolics from digests of polyphenol-rich potato extracts using the Caco-2/HepG2 co-culture system. *Foods, 7*(1), 8. https://doi.org/10.3390/foods7010008

Sangiovanni, E., Piazza, S., Vrhovsek, U., Fumagalli, M., Khalilpour, S., Masuero, D., … Dell'Agli, M. (2018). A bio-guided approach for the development of a chestnut-based proanthocyanidin-enriched nutraceutical with potential anti-gastritis properties. *Pharmacological Research, 134*, 145–155. https://doi.org/10.1016/j.phrs.2018.06.016

Sova, M., & Saso, L. (2020). Natural sources, pharmacokinetics, biological activities and health benefits of hydroxycinnamic acids and their metabolites. *Nutrients, 12*(8), 2190. https://doi.org/10.3390/nu12082190

Srinivasa, C., Mellappa, G., Patil, S. M., Ramu, R., Shreevatsa, B., Dharmashekar, C., … Shivamallu, C. (2022). Plants and endophytes – a partnership for the coumarin production through the microbial systems. *Mycology, 13*(4), 243–256. https://doi.org/10.1080/21501203.2022.2027537

Szwajgier, D., Borowiec, K., & Pustelniak, J. (2017). The neuroprotective effects of phenolic acids: Molecular mechanism of action. *Nutrients, 9*(5), 477. https://doi.org/10.3390/nu9050477

Tekewe, A., Singh, S., Singh, M., Mohan, U., & Banerjee, U. C. (2008). Development and validation of HPLC method for the resolution of drug intermediates: Dl-3-Phenyllactic acid, dl-*O*-acetyl-3-phenyllactic acid and (±)-mexiletine acetamide enantiomers. *Talanta, 75*(1), 239–245. https://doi.org/10.1016/j.talanta.2007.11.004

Tian, X.-J., Yang, X.-W., Yang, X., & Wang, K. (2009). Studies of intestinal permeability of 36 flavonoids using Caco-2 cell monolayer model. *International Journal of Pharmaceutics, 367*(1), 58–64. https://doi.org/10.1016/j.ijpharm.2008.09.023

Wang, L., Chen, Q., Zhu, L., Li, Q., Zeng, X., Lu, L., … Liu, Z. (2017). Metabolic disposition of luteolin is mediated by the interplay of UDP-glucuronosyltransferases and catechol-*O*-methyltransferases in rats. *Drug Metabolism and Disposition, 45*(3), 306–315. https://doi.org/10.1124/dmd.116.073619

Wojdyło, A., Turkiewicz, I. P., Tkacz, K., Nowicka, P., & Bobak, Ł. (2022). Nuts as functional foods: Variation of nutritional and phytochemical profiles and their *in vitro* bioactive properties. *Food Chemistry: X, 15*, Article 100418. https://doi.org/10.1016/j.fochx.2022.100418

Yuan, R., Li, C., Pan, Y., Zhang, Z., Zhu, Y., & Nie, Y. (2022). Antibacterial and hypoglycemic activity of flavonoids in etiolated tissues from fresh-cut Chinese water-chestnuts (*Eleocharis tuberosa*). *Scientia Horticulturae, 297*, Article 110925. https://doi.org/10.1016/j.scienta.2022.110925

Zeng, X., Zheng, Y., He, Y., Zhang, J., Peng, W., & Su, W. (2022). Microbial metabolism of naringin and the impact on antioxidant capacity. *Nutrients, 14*(18), 3765. https://doi.org/10.3390/nu14183765

Zhang, Y., Yang, Z., Liu, G., Wu, Y., & Ouyang, J. (2020). Inhibitory effect of chestnut (*Castanea mollissima* Blume) inner skin extract on the activity of α-amylase, α-glucosidase, dipeptidyl peptidase IV and *in vitro* digestibility of starches. *Food Chemistry, 324*, Article 126847. https://doi.org/10.1016/j.foodchem.2020.126847